Properties study of $LiNbO_3$ lateral field excited device working on thickness extension mode*

Zhang Zhi-Tian(张志甜)[a], Zhang Chao(张 超)[b]†, Wang Wen-Yan(王文炎)[b], Ma Ting-Feng(马廷锋)[a], Liu Yan(刘 岩)[b], and Feng Guan-Ping(冯冠平)[b]

[a] *Department of Precision Instruments and Mechanology, Tsinghua University, Beijing* 10084, *China*
[b] *Research Institute of Tsinghua University in Shenzhen, Shenzhen, Guangdong* 518057, *China*

(Received 16 December 2009; revised manuscript received 24 March 2010)

This paper investigates the properties of thickness extension mode excited by lateral electric field on $LiNbO_3$ by using the extended Christoffel–Bechmann method. It finds that the lateral field excitation coupling factor for a-mode (quasi-extensional mode) reaches its maximum value of 28% on X-cut $LiNbO_3$. The characteristics of a lateral field excitation device made of X-cut $LiNbO_3$ have been investigated and the lateral field excitation device is used for the design of a high frequency ultrasonic transducer. The time and frequency domain pulse/echo response of the $LiNbO_3$ lateral field excitation ultrasonic transducer is analysed with the modified Krimholtz–Leedom–Matthae model and tested using traditional pulse/echo method. A $LiNbO_3$ lateral field excitation ultrasonic transducer with the centre frequency of 33.44 MHz and the –6 dB bandwidth of 33.8% is acquired, which is in good agreement with the results of the Krimholtz–Leedom–Matthae model. Further analysis suggests that the $LiNbO_3$ lateral field excitation device has great potential in the design of broadband high frequency ultrasonic transducers.

Keywords: lateral field excitation, high frequency ultrasonic transducer, $LiNbO_3$, thickness extension mode

PACC: 7760, 4388

1. Introduction

Thickness extension mode has long been used in the design of various kinds of piezoelectric ultrasonic transducers which are widely used in medical imaging, non-destructive testing, underwater detection, etc. The thickness extension mode is commonly excited by electric field along the thickness direction, which is called thickness field excitation (TFE), as shown in Fig. 1(a).

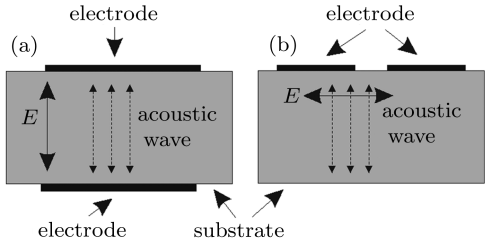


Fig. 1. The configuration of: (a) TFE mode; (b) LFE mode.

Previous studies have found that the acoustic wave could also be excited by lateral electric field with both electrodes only on one side of the piezoelectric substrate,[1−4] which is called lateral field excitation (LFE), as shown in Fig. 1(b). The LFE devices have several attractive advantages.[5] There is no electrode in the region of maximum displacement, which results in higher Q values, better frequency stability and reduced aging of the device. Moreover, the LFE device is slightly thicker than a TFE device for the same resonant frequency,[6] so that LFE device is much easier to achieve high frequency.

In many applications, such as the imaging of eyes, blood vessels, skin and small animals, the high frequency ultrasound imaging system with better resolution is needed.[7,8] Fabrication of the transducers, which is the most critical part of the ultrasound imaging system, becomes more challenging when high frequency and broad bandwidth are required. Previous research on high frequency ultrasonic transducers mostly focused on TFE devices, so that the substrates of these transducers always have electrodes on both sides. Thus, it is hard to fabricate a high frequency ultrasonic transducer with the traditional lapping and dicing method because of the thin substrate (usually less than 100 μm). The special configuration and advantages of LFE device shows its potential in the design of high frequency ultrasonic transducers.

*Project supported by the National Natural Science Foundation of China (Grant No. 60571014) and Shenzhen Shuangbai Project.
†Corresponding author. E-mail: zhangc@tsinghua-sz.edu.cn
© 2010 Chinese Physical Society and IOP Publishing Ltd

Many piezoelectric materials have been investigated for the design of TFE high frequency ultrasonic transducers, such as PZT, $LiNbO_3$, $LiTaO_3$, PMN-33PT, etc. The research had found that $LiNbO_3$ was a suitable material for the design of broadband high frequency TFE ultrasonic transducers due to its high piezoelectric coupling factors.[9] The $LiNbO_3$ is an extremely versatile nonlinear crystal material. Its LFE coupling factors of c-mode (slow shear mode) for all different cut orientations and lateral field directions have been investigated,[10] and the results showed that it has a very high piezoelectric coupling factor. Thus, it is believed that $LiNbO_3$ is also suitable for the design of high frequency LFE ultrasonic transducers. However, the LFE coupling factors of a-mode for all different cut orientations was not presented and no experimental result was given for verifying the LFE properties and its potential use for the design of high frequency ultrasonic transducers.

In the present study, the wave propagation properties of a-mode LFE extensional wave have been investigated for all cut orientations and lateral field directions of $LiNbO_3$. The LFE device on X-cut $LiNbO_3$ has been designed, fabricated and tested. An equivalent circuit model has been used to describe the device's resonance behaviour. The LFE ultrasonic transducer on X-cut $LiNbO_3$ has been designed and tested. The manufacture process of the LFE ultrasonic transducer and experiment setup are revealed in detail. The transducer is tested with the traditional pulse/echo method and detailed analysis of the results is presented.

2. Theory

2.1. Piezoelectric coupling factor

For anisotropic piezoelectric crystals, the piezoelectric coupling factor corresponding to different vibration modes varies with the cut orientation and the applied electric field direction. Piezoelectric coupling factors for the three simple thickness vibration modes (a, quasi-extensional; b, fast-quasi-shear; and c, slow-quasi-shear) of single-crystal piezoelectric plates driven by lateral electric field could be calculated by the extended Christoffel–Bechmann (C–B) method,[11] which assumes that the acoustic plane waves are propagating in a specified direction with respect to the crystallographic axis of the material. The C–B method was used to calculate the LFE piezoelectric coupling factors of $LiNbO_3$ for a-mode in all different cut orientations.

The IEEE standard[12] was adopted to define both the crystal axial set and the notation $(YXwlt)\varphi/\theta/\psi$as shown in Fig. 2, which specifies the orientation of a substrate aligned with a rotated coordinate set of axes. The thickness of the substrate is taken along the rotated Y-axis, which is the direction of acoustic plane wave propagation. From Fig. 2, the substrate is firstly rotated through the angle φ about the Z-axis, then the angle θ about the X-axis, and finally the angle ψ about the Y-axis, which is equal to the angle between the applied electric field direction and X-axis.

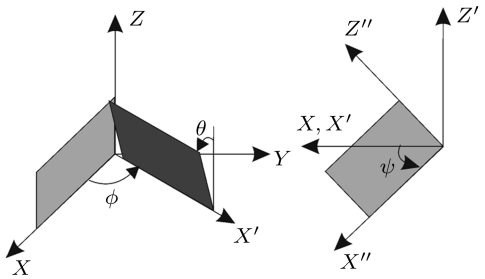


Fig. 2. Notation system used for designating (a) crystallographic orientation of a given substrate, and (b) E-field direction relative to the crystallographic axes.

The material constants of $LiNbO_3$ used in the calculation were referred to Ref. [13]. The calculated results are plotted in Fig. 3. From Fig. 3, $LiNbO_3$ has a maximum LFE coupling factor of 28% for a-mode when $\psi = 7.5°$ and the cut orientation is $(yxw) \pm 30°$ or when $\psi = -7.5°$ and the cut orientation is $(yxw) \pm 90°$ (X-cut), namely $(\varphi, \theta, \psi) = (0°, \pm 30°, -7.5°)$ or $(\varphi, \theta, \psi) = (0°, \pm 90°, 7.5°)$. Thus, the X-cut $LiNbO_3$ was chosen for the design of LFE ultrasonic transducers.

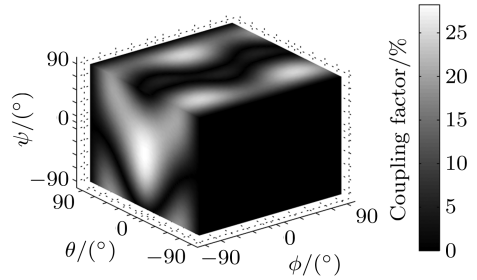


Fig. 3. The LFE piezoelectric coupling factors of $LiNbO_3$ for a-mode in all cut orientations.

The LFE piezoelectric coupling factors of X-cut $LiNbO_3$ for a-, b- and c- modes were calculated with the C–B method and plotted in Fig. 4 as a function of the angle (ψ). It could be found that the coupling

factors of b- and c- modes excited by lateral electric field are zero for all electrical angles on X-cut $LiNbO_3$ and K_a (LFE) reaches its maximum value of 28% at $\psi = 7.5°$, so that a pure LFE a-mode could be excited on X-cut $LiNbO_3$.

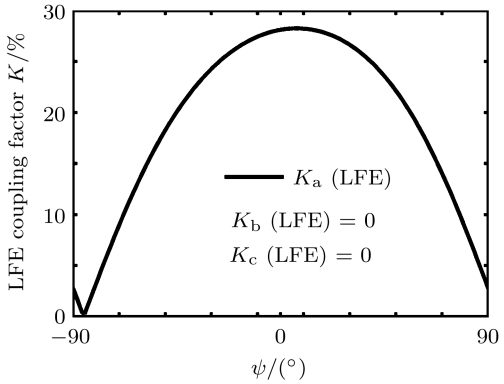


Fig. 4. The LFE piezoelectric coupling factors as a function of the electric field direction angle for X-cut $LiNbO_3$.

2.2. Acoustic wave phase velocity

The phase velocity of the LFE device could be calculated according to the stiffened Christoffel equation,[6]

$$\boldsymbol{k}^2 \left(\boldsymbol{l}_{\mathrm{iK}} \left\{ \boldsymbol{c}^{\mathrm{E}}_{\mathrm{KL}} + \frac{[\boldsymbol{e}_{\mathrm{K}}\boldsymbol{l}_{\mathrm{j}}][l_{\mathrm{i}}e_{\mathrm{iL}}]}{\boldsymbol{l}_{\mathrm{i}}\boldsymbol{\varepsilon}^{\mathrm{S}}_{\mathrm{ij}}\boldsymbol{l}_{\mathrm{j}}} \right\} \boldsymbol{l}_{\mathrm{Lj}} \right) v_{\mathrm{j}} = \rho\omega^2 v_{\mathrm{i}}, \quad (1)$$

where $\boldsymbol{k}$ denotes the wave vector, $\boldsymbol{l}_{\mathrm{iK}}$ denotes the wave propagating direction matrix, $\boldsymbol{l}_{\mathrm{Lj}}$ denotes the transpose of $\boldsymbol{l}_{\mathrm{iK}}$, $\boldsymbol{c}^{\mathrm{E}}_{\mathrm{KL}}$ denotes the stiffness constants matrix under the condition of constant electric field, $\boldsymbol{e}_{\mathrm{K}}$ denotes the piezoelectric stress constants matrix, e_{iL} denotes the transpose of $\boldsymbol{e}_{\mathrm{K}}$, $\boldsymbol{l}_{\mathrm{j}}$ denotes the field direction matrix, $\boldsymbol{l}_{\mathrm{i}}$ denotes the transpose of $\boldsymbol{l}_{\mathrm{j}}$, $\boldsymbol{\varepsilon}^{\mathrm{S}}_{\mathrm{ij}}$ denotes the permittivity constants matrix under the condition of constant strain, v_i denotes the acoustic wave phase velocity, ρ denotes the material density, and ω denotes the angle frequency.

The phase velocity for a-mode of the X-cut $LiNbO_3$ was calculated and plotted in Fig. 5. It can be found that the phase velocity varies between 6550 and 6850 m/s as a function of the driving electric field angle (ψ). When $\psi = 7.5°$, the velocity of a-mode is $v_{\mathrm{a}} = 6829.2$ m/s.

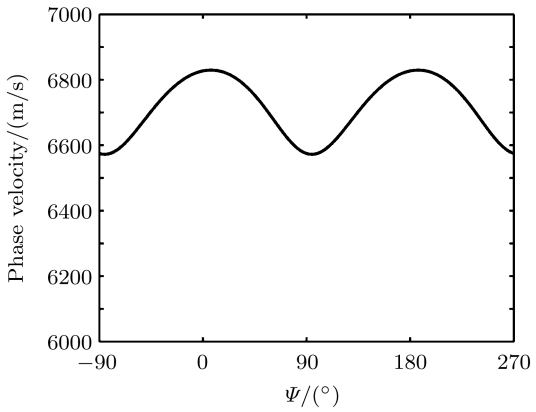


Fig. 5. Phase velocity of the a-mode excited by lateral field on X-cut $LiNbO_3$.

3. Experimental

3.1. Device design

Based on the above calculated results, the LFE device is designed and fabricated by using X-cut $LiNbO_3$, as shown in Fig. 6. The substrate is rectangular with the size of $L \times W = 4$ mm $\times$ 3 mm. Two parallel electrodes with a gap $t = 0.5$ mm were deposited by vacuum evaporation, which consist of a 2 nm thick adhesion layer of chromium followed by 200 nm thick gold. The angle between the direction of the gap and the crystallographic X-axis of the piezoelectric substrate is 82.5° to make sure the electrical angle $\psi = 7.5°$. The thickness of the X-cut $LiNbO_3$ plate d was lapped down to approximately 0.31 mm. The corresponding resonant frequency is (λ denotes the wavelength):

$$f = \frac{v}{\lambda} = \frac{v}{2d} = \frac{6829.2}{2 \times 0.31 \times 10^{-3}} = 11.01 \text{ MHz}. \quad (2)$$

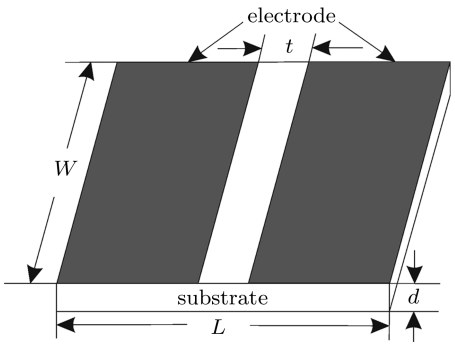


Fig. 6. Detailed configuration of LFE $LiNbO_3$ device.

This $LiNbO_3$ LFE device was used for the fabrication of a high frequency ultrasonic transducer. A 4-mm thick backing layer with 1 part insulating epoxy (EPO-TEK301, Epoxy Tech., Billerica, MA) to 4 part

tungsten powder was firstly cast onto one side (the one has electrodes) of the $LiNbO_3$ LFE device. The acoustic impedance of this backing material is about 5.68 MRayl. Then the $LiNbO_3$ plate was polished down to $d = 0.1$ mm thick, corresponding to the resonant frequency of 34.15 MHz. A quarter wavelength Al_2O_3 epoxy composite matching layer with 1 part insulating epoxy (EPO-TEK301, Epoxy Tech., Billerica, MA) to 1.1 part Al_2O_3 powder was cast onto the barefaced side of the LFE $LiNbO_3$ device. Finally, a quarter wavelength insulating epoxy (EPO-TEK301, Epoxy Tech., Billerica, MA) was cast onto the first matching layer. The acoustic impedances of the first and second matching material are 5.9 MRayl and 2.74 MRayl respectively.

3.2. Experimental setup

The HP4294 impedance analyser was used to test the impedance of the LFE $LiNbO_3$ device. The LFE transducer was tested by using the pulse/echo method in a room temperature degassed water bath. The experimental measurement system is shown in Fig. 7. The Panametrics 5900PR (Olympus NDT inc., Waltham, Ma) was used to excite the transducer. It was set at energy of 32 μJ, gain of 54 dB and filter of 1 MHz–100 MHz. The echo target was a polished quartz plate placed at the focal point of the transducer. The reflected waveforms were received and digitized by an oscilloscope (Tektronix TDS5034, Tektronix Inc. BEAVERTON, OR).

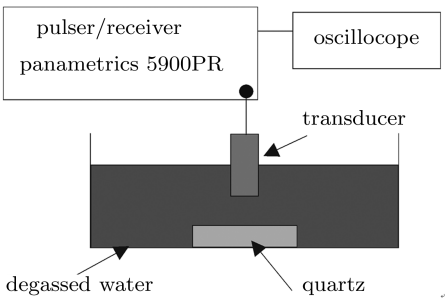


Fig. 7. Experimental measurement system for the measurement of transducer pulse/echo response.

4. Results and discussion

The impedance and phase curve of the $LiNbO_3$ LFE device measured in air are shown in Figs. 8 and 9. It can be seen that the resonance frequency excited by lateral electric field is 10.86 MHz, which is slightly lower than the above calculated result. It is believed that this is resulted by the mass effect of the electrodes.

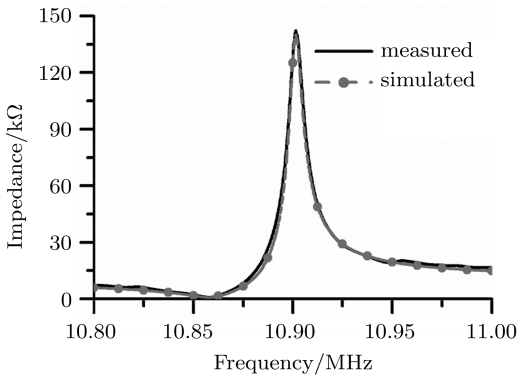


Fig. 8. Impedance vs frequency for the $LiNbO_3$ LFE device.

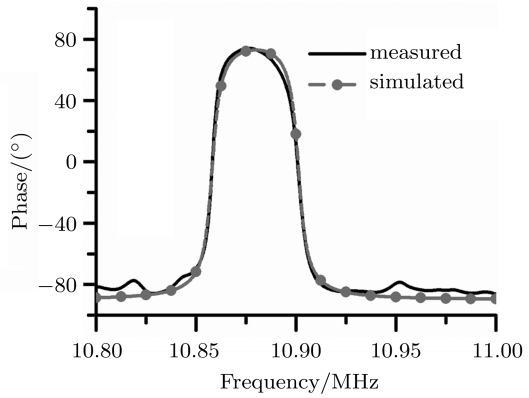


Fig. 9. Phase vs frequency for the $LiNbO_3$ LFE device.

The measured impedance and phase curve can be equivalent with the characteristic curve of a common BVD (Butterworth–Van Dyke) circuit, as shown in Fig. 10, which is well known in the description of a thickness shear mode (TSM) resonator's behaviour. When $R_m = 780\ \Omega$, $L_m = 19.2$ mH, $C_m = 11.2$ fF, and $C_0 = 1.4$ pF, the simulated impedance and phase curve are almost identical to the measured ones, as shown in Figs. 8 and 9. This result shows that both TFE and LFE devices have the same equivalent circuit configurations. Thus, the Krimholtz–Leadom–Matthae (KLM) transmission line model[14] of TFE device could also be used for LFE device. The only difference is the calculation of C_0, which is caused by the different electrode configurations of TFE and LFE devices.

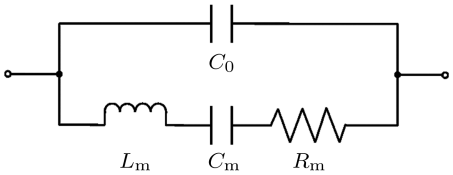


Fig. 10. The BVD equivalent circuit of the $LiNbO_3$ LFE device.

The KLM transmission line model of the $LiNbO_3$ LFE device is shown in Fig. 11. According to the calculation of C_0 in the BVD equivalent circuit,[6] the elements of the KLM model could be calculated by these following equations:

$$C_0 = \frac{\varepsilon W d}{t}, \tag{3}$$

$$C = -MC_0/[k_t^2 \sin c(\omega/\omega_0)], \tag{4}$$

$$\psi = Mk_t(\pi/\omega_0 C_0 Z_0)^{1/2} \sin c(\omega/2\omega_0). \tag{5}$$

$$M = Lt/\left\{d^2\left[1 + k_t^2 \tan(\pi\omega/\omega_0)/(\pi\omega/\omega_0)\right]\right\}. \tag{6}$$

Where ε denotes the permittivity of the piezoelectric plate, W, d, t L denote the dimension of the LFE device as shown in Fig. 6, k_t denotes the LFE piezoelectric coupling factor, ω, ω_0 denote the angle frequencies, Z_0 denotes the acoustic impedance of the piezoelectric plate.

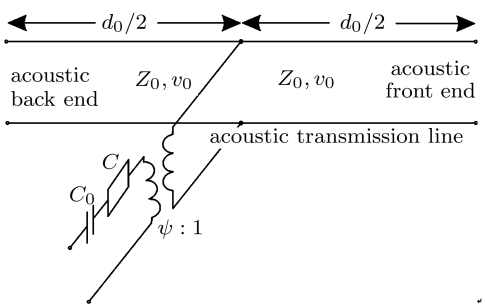


Fig. 11. The KLM transmission line model of the $LiNbO_3$ LFE device.

With this KLM transmission line model, the time and frequency domain pulse/echo response of the LFE ultrasonic transducer could be calculated as the same as the TFE ultrasonic transducers.[15] The simulated time and frequency domain pulse/echo response curve are shown in Fig. 12. The result shows that the central frequency of the transducer is 33.3 MHz and the –6 dB bandwidth is 33.4%.

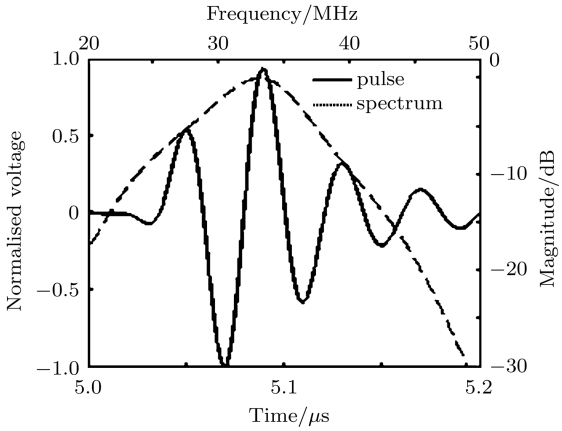


Fig. 12. Modeled time and frequency domain pulse/echo response of the LFE $LiNbO_3$ ultrasonic transducer.

The measured and normalised pulse/echo waveform of the $LiNbO_3$ LFE ultrasonic transducer is shown in Fig. 13(a). The spectral analysis of this curve was done with MATLAB and shown in Fig. 13(b). It can be found that the –6 dB bandwidth of this LFE ultrasonic transducer is 33.8% and the central frequency is 33.44 MHz. The experimental result is in good agreement with the result of the KLM transmission line model. The central frequency is slightly lower than the resonant frequency (34.15 MHz). This is caused by the load effects of backing and matching layers.

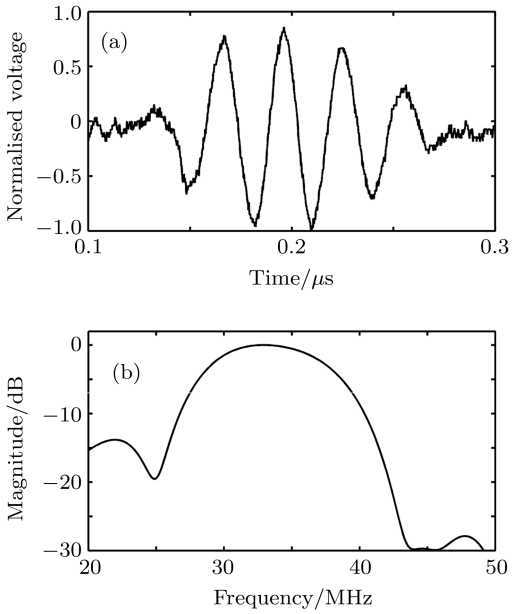


Fig. 13. Normalised time and frequency domain pulse/echo response of the $LiNbO_3$ LFE ultrasonic transducer.

The bandwidth of the $LiNbO_3$ LFE ultrasonic transducer is relatively lower. This is due to the poor matching between X-cut $LiNbO_3$ and water. The bandwidth can be improved further with the optimisation of acoustic matching layers. Further theory analysis with the KLM transmission line model showed that the bandwidth of the LFE $LiNbO_3$ ultrasonic transducer could be increased to 70.9% if the first matching layer impedance increases to 9 MRayl, as shown in Fig. 14. Thus, $LiNbO_3$ has great potential in the design of high frequency broadband LFE ultrasonic transducers.

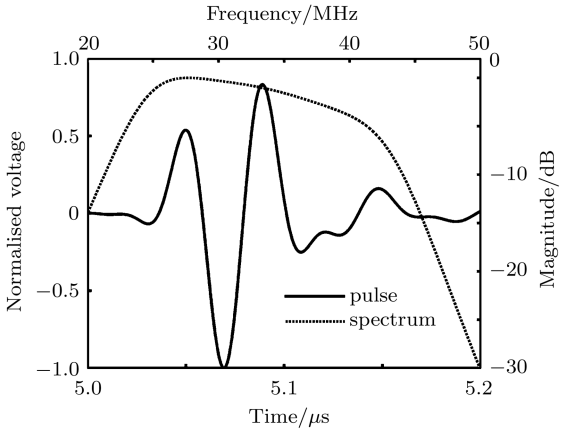


Fig. 14. Modeled time and frequency domain pulse/echo response for LFE $LiNbO_3$ ultrasonic transducer with better matching scheme.

5. Conclusions

The properties of thickness extension mode excited by lateral electric field on $LiNbO_3$ have been investigated. It is found that the LFE coupling factors for a-mode have the maximum value of 28% when the cut orientation of $LiNbO_3$ is X-cut and the electric field angle $\psi = 7.5°$. The phase velocity of the extensional wave varies between 6550 and 6850 m/s as a function of the driving electric field angle (ψ). The X-cut $LiNbO_3$ was chosen for the design of an LFE device and a high frequency ultrasonic transducer. The KLM transmission line model was modified to simulate the time and frequency domain pulse/echo response of LFE ultrasonic transducers. The characteristic of the $LiNbO_3$ LFE ultrasonic transducer was predicted with the KLM transmission line model. The experimental results showed that the central frequency of the ultrasonic transducer is 33.44 MHz and the –6 dB bandwidth is 33.8%, which is in good agreement with the result of the KLM transmission line model. Further analysis predicts that $LiNbO_3$ is a good material for the design of high frequency broadband LFE ultrasonic transducers.

References

[1] Hu Y, Pinkham W, French Jr L A, Frankel D and Vetelino J F 2005 *Sensors and Actuators* B: *Chemical* **108** 910

[2] Wang W, Zhang C, Zhang Z, Liu Y and Feng G 2008 *Appl. Phys. Lett.* **93** 242906

[3] Hu Y, French Jr L A, Radecsky K, Da Cunha M P, Millard P and Vetelino J F 2004 *IEEE Trans. on Ultrasonics, Ferroelectrics, and Frequency Control* **51** 1373

[4] York C, French L A, Millard P and Vetelino J F 2005 *IEEE International Ultrasonics Symposium* Rotterdam, Netherlands, Sep.18- 2005 p44–49

[5] Ballato A, Hatch E R, Mizan M and Lukaszek T J 1986 *IEEE Trans. on Ultrasonics, Ferroelectrics, and Frequency Control* **33** 385

[6] Rosenbaum J F 1988 *Bulk Acoustic Wave Theory and Devices* (Boston, MA: Artech House)

[7] Lockwood G R, Lockwood G R, Turnball D H, Christopher D A and Foster F S A F F S 1996 *Engineering in Medicine and Biology Magazine, IEEE* **15** 60

[8] Zipparo M J, Shung K K and Shrout T R 1997 *IEEE Trans. on Ultrasonics, Ferroelectrics and Frequency Control* **44** 1038

[9] Cannata J M, Ritter T A, Wo-Hsing C and Shung K K 2000 *Ultrasonics Symposium, Vol.2 2000 IEEE* 2000 1129–1133

[10] Wang W Y, Zhang C, Zhang Z T, Liu Y and Feng G P 2009 *Chin. Phys.* B **18** 795

[11] Khan A and Ballato A 2002 *IEEE Trans. on Ultrasonics, Ferroelectrics, and Frequency Control* **49** 922

[12] IEEE 1987 *ANSI/IEEE standard* 176-1987

[13] Auld B A 1973 *Acoustic Fields and Waves in Solids* (Volume I) (New York: Wiley)

[14] Krimholtz R, Leedom D A and Matthaei G L 1970 *Electron. Lett.* **6** 398

[15] Cannata J M and Shung K K 2003 *2003 IEEE Symposium on Ultrasonics* October 5–8 2003, Honolulu, Hawail, USA 1658